MASTER OF PHILOSOPHY, Modelling of Materials

Thursday 25 April 2002 **9 – 12**

MODELLING OF MATERIALS (1) – possible Answers

SECTION A

1. (a)

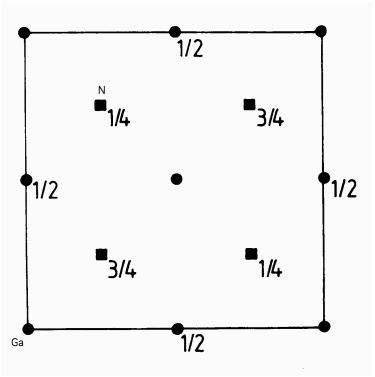

(b) Atomic ordering is favoured in systems where the enthalpy of mixing is negative. However, there is also an increase in free energy due to a reduction in entropy as disorder is replaced by order. As the temperature increases, the free energy increase caused by the reduced entropy of ordering dominates, because it scales with T (*i.e.* $\Delta G = \Delta H - T\Delta S$). This is why disordering occurs as the temperature is increased.

(c) Main point: synergy means a coupled approach intended to produce a more reliable result than any of the individual methods would alone. There is an interplay between theory, modelling and experiment. Each approach can provide support for the other two. Modelling should not be performed in a vacuum. Experimental observation should be connected to an established theory or computer model.

This approach serves to validate the model (or theory) and confirm the interpretation of the experiment.

A coupled approach is possible now because of a convergence of capabilities: improved theories, more efficient algorithms, more powerful computers, more sophisticated experimental tools.

"materials by design" the use of a coupled approach to guide in the design of a material with specific properties (*e.g.* high strength, high conductivity, efficient luminescence).

"ab initio materials science" the use of a first principles model (involving no parametric fitting) to explain or predict a phenomenon in materials science.

"intelligent processing of materials" the use of a coupled approach to process materials optimally.

(d) The Ziman model considers the reflection of electron waves from a crystal lattice represented by a periodic crystal potential.

The band gaps originate from the constructive interference between electron (or Bloch) waves in the material as they are reflected by this potential.

For critical values of the wave vector given by the Bragg condition, the Bloch waves change from being travelling waves to being standing waves.

Travelling wave solutions to the Schrodinger equation therefore do not exist at the Bragg condition, i.e. on the Bragg planes or Brillouin zone boundaries, and there is a gap in the allowed electron energy levels.

At $k = \pm n\pi/a$ (the Bragg condition in 1–D where a is the lattice spacing), it can be shown that the two standing waves have different charge densities proportional to $\cos^2(\pi x/a)$ and $\sin^2(\pi x/a)$ and thus two different energies. This creates the discontinuity in the electron energy spectrum.

(e)

```
      real function trace (a, b)
      real sum
      real a(3,3), b(3,3)
      integer i, k
      sum = 0.0
      do 10, i = 1, 3
         do 10, k = 1, 3
            sum = sum + a(i,k) * b(k,i)
10    continue
      trace = sum
      return
      end
```

(f) Since, $\Delta S^\circ \simeq -\Delta S^\circ_{O_2}$ for the oxidation reaction is a negative quantity, and the standard free energy change for the above reaction is given by: $\Delta G^\circ = \Delta H^\circ - T\Delta S^\circ$, as T is increased, the value ΔG° also increases.

(g) The grand partition function is defined as the sum of the Boltzmann factors over all microstates of an atomistic system Z. The formal definition as below (β is $1/k_B T$, E_i is energy of microstate, μ is chemical potential and n_i is number of particles in each microstate):

$$Z = \sum_i \exp\{-\beta(E_i - \mu n_i)\}$$

Although every thermodynamic state function can in principle be calculated from the derivatives of Z, the energy of each microstate could potentially be a function of the position and velocity of every particle in the system. This makes the calculation of expectation values of the state functions, which determine materials properties, intractable in practice even if the partition function is known in full.

An alternative method is to use computer simulation to sample the microstates of the system. As the total number of states of real systems is huge, the sampled states must be representative of those of the real system. In the Monte Carlo method, this is achieved by sampling microstates with a probability proportional to their Boltzmann factor. In the molecular dynamics method, Newton's equations of motion are solved for a system in equilibrium with a heat and particle reservoir. In both cases, the expectation values of the state functions are given by simply averaging over the sampled states. Extra marks for including proviso that if the simulations are ergodic, averaging over configurations in MC and over time in MD should give the same answer.

(h) A mesoscale level can be defined if at that length (and associated time) scale one can safely make the assumption that certain degrees

of freedom pertaining to a smaller scale will always be in the equilibrium state when seen from that scale, *i.e.* have a relaxation time much shorter than the time scale of interest.

A common example of a mesoscopic phenomenon is Brownian motion. This can be observed in small soot particles viewed under the microscope, where the net result of small, uncorrelated collisions of gas molecules cause the soot particles to execute random motion with a mean–squared displacement which is proportional to the time period of observation, as predicted by Einstein. Although the soot particle is thermally equilibrated with respect to the fast motions of the gas molecules, the observations occur over a much longer time scale and so Brownian motion provides a direct link between the microscopic jumps of the particle and its macroscopic diffusivity. It can occur in any physical situation in which a process is observed over a sufficiently long time scale that the microscopic degrees of freedom have time to equilibrate.

(i) The Deborah number gives the ratio of the longest relaxation time of the polymer to the time scale of the process. Under the conditions described, the process is an order of magnitude slower than the relaxation time, and so the flow through the die will be viscous. This means that the swelling of the extrudate should be fairly isotropic, as the polymer has no memory of its previous configuration. However, tripling the molecular weight will increase the viscosity, and therefore the relaxation time. Since the molecular weight is already high enough so that the polymer melt is entangled then $\eta \propto M^{3.3}$, so the viscosity will increase by a factor of $3^{3.3} = 37.5$. This will change the Deborah number to 3.75, resulting in an elastic flow through the die. The polymer melt will retain a memory of its configuration before compression, and there is likely to be appreciable die swell.

(j) There is in general a change in density or electrical resistance during a phase transformation. This can be used to monitor transition temperatures or pressures in pure systems. In alloys, the chemical composition of the phases in equilibrium does not change with the overall composition. The lattice parameters can be monitored (using X–ray, electron or neutron diffraction) as a function of the overall composition; a lack of change indicates phases in equilibrium, where only their proportions change according to the lever rule.

The chemical compositions of phases can also be monitored directly using the variety of microanalytical techniques available in modern electron–optical instruments (energy dispersive X–ray analysis, wavelength dispersive X–ray analysis, electron energy loss spectroscopy *etc.*).

Thermodynamic data (heat capacity, enthalpy changes) can be measured using calorimetry (differential scanning calorimetry or differential thermal analysis). These can then be used to construct databases which are analysed using solution models to construct phase diagrams.

SECTION B

2. Taylor series expansions about the point x_i

$$T_{i+1} = T_i + \Delta x T_i' + \frac{\Delta x^2}{2!} T_i'' + \frac{\Delta x^3}{3!} T_i''' + \ldots$$
$$T_{i-1} = T_i - \Delta x T_i' + \frac{\Delta x^2}{2!} T_i'' - \frac{\Delta x^3}{3!} T_i''' + \ldots$$

on adding these equations, rearranging and truncating the series gives a central difference approximation

$$T_i'' = \frac{T_{i+1} - 2T_i + T_{i-1}}{\Delta x^2}$$

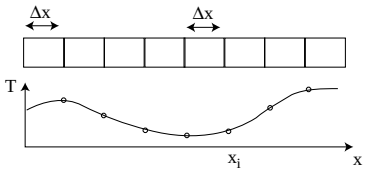

The 1–D Fourier (heat conduction) equation

$$\frac{\partial T}{\partial t} = \alpha \frac{\partial^2 T}{\partial x^2}$$

can be written in finite difference form by using forward and central difference approximations for the two derivatives:

$$\frac{T_{i,j+1} - T_{i,j}}{\Delta t} = \alpha \left[\frac{T_{i,j+1} - 2T_{i,j} + T_{i-1,j}}{\Delta x^2} \right]$$

which leads to the explicit recurrence relation:

$$T_{i,j+1} = T_{i,j} + \frac{\alpha \Delta t}{\Delta x^2} \left[[T_{i+1,j} - 2T_{i,j} + T_{i-1,j} \right]$$

The equation can be written:

$$T_{i,j+1} = A\big(T_{i+1,j} + T_{i-1,j}\big) + (1 - 2A) T_{i,j}$$

where A is given by $\alpha \Delta t / \Delta x^2$. It is clear that $(1 - 2A)$ should not be negative, since this would mean that an increase in the current value of T at a particular point would decrease the new value at that point, which would lead to oscillations. A criterion for numerical stability therefore

arises with an explicit solution scheme, which corresponds to a maximum value being imposed on the time increment:

$$\Delta t \leq \frac{\Delta x^2}{2\alpha}$$

A physical interpretation of how numerical instability arises if this condition is not satisfied is that Δt is then so long that the heat flow, which should act to reduce the curvature of the temperature profile, over–corrects and starts to reverse the sign of the curvature. This is physically impossible. It arises because, in an explicit scheme, the temperature of each element is assumed to stay at its current value until the end of the time increment.

3. Thermal history is important as follows:

• in maximising throughput (*e.g.* to check that increases in speed do not lead to problems): *e.g.* in DC casting it is necessary to avoid going too fast and causing a "break-out" of molten metal;

• in controlling thermally-induced stresses, which lead to billet end-cracks in DC casting and distortion/warpage/cracking in extrusion

• in controlling microstructure evolution: *e.g.* dendrite spacing, grain size and segregation in DC casting; full dissolution during extrusion, and avoidance of coarse precipitation during subsequent cooling (quench sensitivity).

Numerical methods are particularly necessary to capture the following:

• in DC casting: many materials in the problem (liquid and solid aluminium, steel starting block, copper mould) and complex thermal boundary conditions (liquid and solid against copper mould, water quench, turning to steam)

• in extrusion: complex 3D geometry of the extruded profile and the interior cavity in the die, giving complex metal flow paths; also contact with steel dies (friction and heat transfer) followed by some combination of air and water cooling.

Refinements to the Jominy model for greater accuracy:

• more elements in the length direction, and grade the mesh to be finer near the quenched end where cooling rates are high;

• axisymmetric mesh with a few elements across the radius, to allow for some radial heat flow and convective/radiative heat transfer on the sides of the bar; temperature-dependent thermal properties;

• good but not perfect heat transfer boundary condition on quenched end (with a suitable heat transfer coefficient);

• adjust time stepping to give temperature values which are sufficiently close together in time (at the positions of interest) to give a smooth temperature-time profile.

Transformations to ferrite, pearlite and bainite occur in the higher temperature region (the nose of the C–curve). Avoiding these transformations to produce martensite is the purpose of the quench, so it is in this area that greatest accuracy is needed. These transformations usually do not occur below 350 °C, so accurate cooling histories are not important.

4. The three examples might include: nucleation of crystals in liquid, relevant for metal casting in which equiaxed grains are preferred; intragranular nucleation of acicular ferrite in a solid–state transformation; and nucleation of magnetic domains, relevant for ease of reversal of magnetisation.

The work of formation W of a critical nucleus is given by

$$W = (4\pi/3)r^3\Delta G_V + 4\pi r^2\sigma$$

where ΔG_V is taken to be a positive quantity. This form has a maximum value of W at $r^* = 2\sigma/\Delta G_V$, a value readily found by setting $\partial W/\partial r = 0$. The critical radius is r^* because clusters smaller than this diameter just dissolve, while larger clusters can grow naturally.

Homogeneous nucleation takes place without any pre–existing substrate; heterogeneous nucleation occurs on a substrate, and a drawing of a spherical cap nucleus would be an expected part of the answer. The contact angle of the spherical cap is important in determining the ease of nucleation. The critical radius of curvature of the solid–liquid interface is the same for heterogeneous as for homogeneous nucleation under the same conditions, but the volume of the heterogeneous nucleus is less, reducing the critical work of nucleation W^*. Heterogeneous nucleation is dominant because systems in industrial processing offer many potential substrates.

Problems in quantitative modelling are lack of precision in the values of input parameters, notably in the values of σ. Modelling approaches include use of standard macroscopic values of ΔG_V and σ, use of the density functional to calculate W^*, and use of molecular dynamics to probe nucleation kinetics.

5. The DREIDING force field contains three different types of bonded (or intramolecular) forces: bond stretching, bond bending and bond torsion. Bond stretching forces are defined between each pair of bonded atoms, and are approximated by a harmonic function with an equilibrium separation and force constant. They describe the force required to displace the bonded atoms from their equilibrium separation. Bond bending forces are defined between each triplet of bonded atoms, and are approximated by a harmonic function with an equilibrium bond angle

and force constant. They describe the force required to change the bond angle from its equilibrium value. Bond torsions are defined between each quartet of bonded atoms, and are approximated by a sinusoidal function with a number of different force constants and phase shifts depending on the macromolecule being simulated. They describe the force required to change the dihedral angle between the atoms, which normally has three minimum energy states (one *trans*, two *gauche*).

The parameters of the intramolecular force field terms can be determined from experimental measurements and *ab initio* quantum calculations, and it turns out that there is a wide spread in frequency between the degrees of freedom involving different numbers of atoms. That is, the bond stretching motions are faster than the bond bending, which are faster than the bond torsions. This makes it possible to achieve a saving in efficiency if the slower forces are evaluated using a longer time step than the faster forces. This is the principle of a multiple time step algorithm, in which the slower degrees of freedom of a macromolecule are evolved in the mean field of the faster varying ones. The separation is only rigourously accurate if the different degrees of freedom are truly independent, but it is a good approximation for most systems.

For a graphene sheet comprised of N independent atoms, there are $3N/2$ distinguishable bond stretching terms, $3N$ bending terms and $6N$ torsional terms, giving $21N/2$ bonded terms in total. Using the MTA, the torsional terms are evaluated 50 times less often and the angle terms 10 times less often than the bond stretching terms. This gives a factor of f time saving, where:

$$f = \frac{21N}{2} \times \left(\frac{6N}{50} + \frac{3N}{10} + \frac{3N}{2} \right)^{-1} = 5.47$$

SECTION C

6. For a binary (A–B) solution the numbers of the different kinds of bonds can be calculated using simple probability theory. Given a concentration x of B and a lattice coordination number z, and the fact that the probability of finding a B atom in a random solution is x, it follows that

$$\begin{aligned} N_{AA} &= z\frac{1}{2}N(1-x)^2 \\ N_{BB} &= z\frac{1}{2}Nx^2 \\ N_{AB} + N_{BA} &= zN(1-x)x \end{aligned} \tag{1}$$

where N_{AB} represents both A–B and B–A bonds which cannot be distinguished. N is the total number of atoms. Notice that the unlike bonds A–B and B–A cannot be distinguished and hence have been consolidated.

An ideal solution is one where the atoms mix at random because there is no enthalpy change on mixing (ΔH_M) the components (Table 1). The configurational entropy of mixing is (ΔS_M) is easily derived because the probabilities can be estimated assuming a random distribution of atoms. The enthalpy of mixing is finite for a regular solution, so that the atoms at low temperatures may not be randomly mixed. Nevertheless, as a convenient approximation, the entropy of mixing is assumed to be ideal. A quasichemical model avoids this latter approximation. Note that the regular solution may be considered as a zeroth approximation quasichemical model.

Type	ΔS_M	ΔH_M
Ideal	Random	0
Regular	Random	$\neq 0$
Quasichemical	Not random	$\neq 0$

Table 1: Elementary thermodynamic properties of solutions

Consider an alloy consisting of two components A and B. For the phase α, the free energy will in general be a function of the mole fractions $(1-X)$ and X of A and B respectively:

$$G^\alpha = (1-X)\mu_A + X\mu_B \tag{2}$$

where μ_A represents the mean free energy of a mole of A atoms in α. The term μ is called the *chemical potential* of A, and is illustrated in

Fig. 1a. Thus the free energy of a phase is simply the weighted mean of the free energies of its component atoms. Of course, the latter varies with concentration according to the slope of the tangent to the free energy curve, as shown in Fig. 1.

Consider now the coexistence of two phases α and γ in our binary alloy. They will only be in equilibrium with each other if the A atoms in γ have the same free energy as the A atoms in α, and if the same is true for the B atoms:

$$\mu_A^\alpha = \mu_A^\gamma$$

$$\mu_B^\alpha = \mu_B^\gamma$$

If the atoms of a particular species have the same free energy in both the phases, then there is no tendency for them to migrate, and the system will be in stable equilibrium if this condition applies to all species of atoms. Since the way in which the free energy of a phase varies with concentration is unique to that phase, the *concentration* of a particular species of atom need not be identical in phases which are at equilibrium. Thus, in general we may write:

$$X_A^{\alpha\gamma} \neq X_A^{\gamma\alpha}$$

$$X_B^{\alpha\gamma} \neq X_B^{\gamma\alpha}$$

where $X_i^{\alpha\gamma}$ describes the mole fraction of element i in phase α which is in equilibrium with phase γ *etc.*

The condition the chemical potential of each species of atom must be the same in all phases at equilibrium is quite general and obviously justifies the common tangent construction illustrated in Fig. 1b.

Diffusion is driven by gradients of chemical potential (*i.e.* free energy) rather than chemical concentration. By analogy with Fick's first law:

$$J_A = -M_A \frac{\partial \mu_A}{\partial x} \qquad \text{so that} \qquad D_A = M_A \frac{\partial \mu_A}{\partial C_A}$$

where the proportionality constant M_A is known as the mobility of A. In this equation, the diffusion coefficient is related to the mobility by comparison with Fick's first law.

The relationship is remarkable: if $\partial \mu_A / \partial C_A > 0$ then the diffusion coefficient is positive and the chemical potential gradient is along the same direction as the concentration gradient. However, if $\partial \mu_A / \partial C_A < 0$ then the diffusion will occur against a concentration gradient.

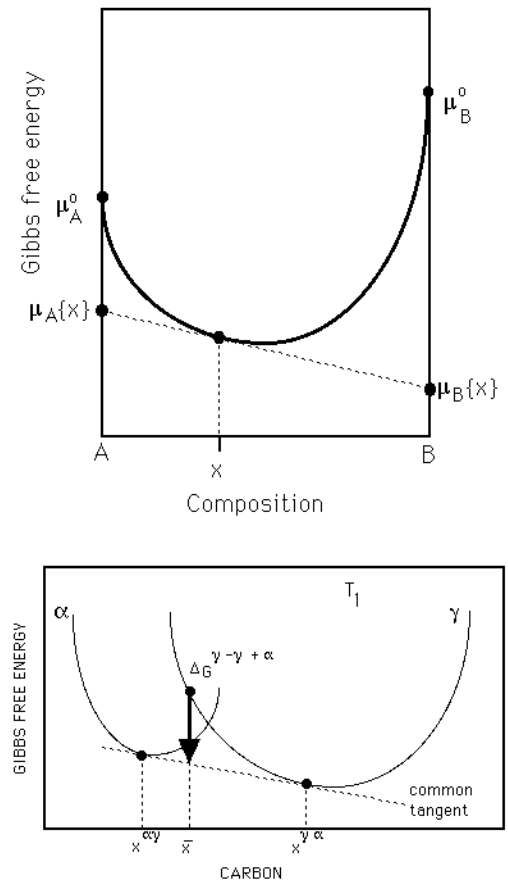

Fig. 1: (a) Diagram illustrating the meaning of a chemical potential μ. (b) The common tangent construction giving the equilibrium compositions of the two phases at a fixed temperature.

7. **Assumptions**:

(i) Solid is modelled as a gas of negatively charged electrons plus a positively charged background charge (a jellium). The background charge serves to maintain charge neutrality.

(ii) Explicit electron–ion interactions are ignored (the free electron approximation).

(iii) Explicit electron–electron interactions are ignored (the independent electron approximation).

Quantisation of the electron energies: Let the jellium be contained in a box of side L. From wave–particle duality, the free electrons have wave functions ψ and satisfy the following wave equation:

$$\frac{\hbar^2}{2m}\nabla^2\psi(r) = -E\psi(r)$$

where E are the electron energy eigenvalues. By substitution it can be seen that solutions of this equation have the form:

$$\psi(r) = C^{i\mathbf{k}.\mathbf{r}}$$

where $\mathbf{k}$ is a vector normal to the wavefront with magnitude $k = \sqrt{2mE}/\hbar$.

Periodic boundary conditions are now applied to the box. This confines the electrons to the box and avoids unwanted surface effects. It also leads to travelling (rather than standing) wave solutions which are better for describing charge transport properties.

The boundary conditions require that

$$\begin{aligned}\psi(x, y, z + L) &= \psi(x, y, z)\\ \psi(x, y + L, z) &= \psi(x, y, z)\\ \psi(x + L, y, x) &= \psi(x, y, z)\end{aligned}$$

and must satisfy $\psi(x, y, z) = Ce^{i(k_x x + k_y y + k_z z)}$, *i.e.* $e^{ik_x L} = e^{ik_y L} = e^{ik_z L}$ so that

$$k_x = \frac{2\pi n_x}{L}, \qquad k_y = \frac{2\pi n_y}{L}, \qquad k_z = \frac{2\pi n_z}{L}, \qquad \text{where } n \text{ is an integer}$$

Hence k is quantised and so therefore is $E(k)$.

The Fermi Energy: the quantised wavevector $\mathbf{k} = (k_x, k_y, k_z)$ defines a 3–D reciprocal space. In this k–space all allowed electron energies fall within a sphere of radius k_F (the magnitude of the Fermi vector).

The spacing between k points is $2\pi/L$. Thus the volume per k–point is $(2\pi/L)^3$. Therefore the volume of the Fermi sphere of radius k_F is $\frac{1}{2}N\frac{(2\pi)^3}{V}$ where the factor of a half accounts for the fact that 2 electrons can occupy each k state, N is the number of electrons in the box and $V = L^3$. Thus

$$\frac{1}{2}N\frac{(2\pi)^3}{V} = \frac{4}{3}\pi k_F^3 \qquad \text{so that}$$
$$k_F = (3\pi^2 n_c)^{1/3} \quad \text{where} \quad n_c = N/V \text{ (the electron density)}$$

Hence the Fermi energy becomes

$$E_F = \frac{\hbar^2 k_F^2}{2m} = \frac{\hbar^2}{2m}(3\pi^2 n_c)^{\frac{2}{3}}$$

The Fermi Energy of Copper: For Cu, the electron density is given by

$$n_c = \frac{(4 \text{ atoms/cell})(1 \text{ electron/atom})}{(3.62 \times 10^{-10})^3} = 8.432 \times 10^{28}\,\text{m}^{-3}$$

Hence by substitution $E_F = 1.12 \times 10^{-18}\text{J} \equiv 7.01\text{eV}$

The Fermi wavelength of Copper: The magnitude of the wave vector is $k_F = (3\pi^2 n_c)^{\frac{1}{3}}$. The Fermi wavelength is therefore $\lambda_F = 2\pi/k_F = 0.46\,\text{nm}$.

The Fermi velocity of Copper: Use de Broglies relation, momentum $p = h/\lambda$. Hence the Fermi velocity $v_F = \frac{p_f}{m} = \frac{h}{m\lambda_F} = \frac{2\pi\hbar}{m\lambda_F} = 1.57 \times 10^6\,\text{m}\,\text{s}^{-1}$.

Failure of the Free Electron Model: The model works quite well for metals because it is assumed that the density of electrons is uniform. This is the case, at least for simple metals, and accounts for a wide range of metallic properties, for example, good electrical and thermal conductivity, close–packed structures (no directional bonding) and ductility (uniform density).

It fails for other classes of materials, *e.g.* semiconductors and insulators, because here the valence electron density is not uniform (in semiconductors it is localised along certain directions and in insulators it is localised around the atoms). In order to predict the non–localisation of electron density, crystal structure has to be incorporated into the model. This leads to a fragmentation of the electron energy spectrum and the appearance of allowed bands of energy separated by gaps of forbidden energy.

Thus one property of a semiconductor that the free electron model cannot predict is the observed band gap (*e.g.* 1 eV in Si). The presence of a band gap affects all other electronic and optical properties of semiconductors, *e.g.* the dependence of conductivity on doping and temperature, the wavelength of emitted light in LEDs and lasers.

The effect of a periodic crystal potential: The incorporation of crystal structure into the model means that the electrons will interact with a periodic crystal potential. It can be shown that for certain critical values of the electron wave vectors, the crystal potential will reflect the electrons such that the incident and reflected waves interfere constructively. In this situation, the electron travelling waves of a single energy split into two standing waves with different energies. One standing wave concentrates electrons on the atoms while the other standing wave concentrates electrons in the space between atoms (this can be shown mathematically by considering the probability density of each wave but this is not asked for in the question). The energy of the standing wave which concentrates electrons between the atoms will be higher than the standing wave which concentrates electrons on the atoms since the crystal potential is strongest between the atoms. Thus for the critical wave vectors, the electron energies will assume two values, one higher than the free electron value and one lower than the free electron value. This creates a discontinuity in the electron energy spectrum at these k-vectors, which collectively form

a plane in k–space known as a Brillouin zone boundary.

Electron energy spectrum near a BZ boundary: